Dental Journal
Majalah Kedokteran Gigi

Dental Journal
(Majalah Kedokteran Gigi)
2023 September; 56(3): 144–153

Original article

Ovalbumin's potential as a wound-healing medicament in tooth extraction socket by induction of cell proliferation through the ERK2 pathway in silico

Sri Nabawiyati Nurul Makiyah[1], Sartika Puspita[2]
[1]Department of Histology and Cell Biology, School of Medicine, Faculty of Medicine and Health Sciences, Universitas Muhammadiyah Yogyakarta, Yogyakarta, Indonesia
[2]Department of Oral Biology, School of Dentistry, Faculty of Medicine and Health Sciences, Universitas Muhammadiyah Yogyakarta, Yogyakarta, Indonesia

ABSTRACT

Background: *The trend of studies on dental medicaments is increasing rapidly. Antibacterial or anti-inflammatory activity is most frequently studied. Ovalbumin is one of the proteins whose benefits have been studied, but these benefits are still limited because of ovalbumin's potential for proliferative bioactivity.* ***Purpose:*** *The aim of this study is to examine ovalbumin's potential as a wound-healing medicament through molecular docking analysis on a protein related to the extracellular signal-regulated kinases/mitogen-activated protein kinase (ERK/MAPK) signaling pathway.* ***Methods:*** *Ovalbumin was hydrolyzed through BIOPEP-UWM (The BIOPEP-UWM™ database of bioactive peptides). Protein target and interaction were predicted using Similarity Ensemble Approach target prediction webserver, SuperPred webserver, STRING webserver, and Cytoscape version 3.9.1. Selected fragments were docked using Autodock Vina in PyRx 0.8 with Tukey's multiple comparison test and Biovia Discovery Studio version 19.1.0.18287 for visualization.* ***Results:*** *This study found that ovalbumin has the potential to positively regulate cell proliferation, angiogenesis, and fibroblast growth factor production. Six of the 131 fragments of ovalbumin could interact with 73 proteins, and the 20 proteins with the highest probability and score of betweenness centrality showed potential for bioactivity. Five fragments and povidone-iodine interacted inside the Adenosine triphosphate (ATP) phosphorylation site of ERK2, whereas fragment 1 (F1) and glycerin interacted outside the site. F1 could decrease the binding energy required for adenosine 5'-[,-methylene]triphosphate or an ATP-analogue chemical compound to interact with ERK2 compared to the control, with a score that was not significant.* ***Conclusion:*** *Ovalbumin has the potential to induce cell proliferation by affecting ERK2-ligand interactions.*

Keywords: *angiogenesis; cell proliferation; ERK2; MAPK; ovalbumin*
Article history: *Received 14 October 2022; Revised 6 December 2022; Accepted 14 February 2023; Published 1 September 2023*

Correspondence: Sri Nabawiyati Nurul Makiyah, Histology and Cell Biology Department, School of Medicine, Faculty of Medicine and Health Sciences, Universitas Muhammadiyah Yogyakarta, Brawijaya Street, Tamantirto, Kasihan, Bantul, Yogyakarta, 55183 Indonesia. Email: nurul.makiyah@umy.ac.id

INTRODUCTION

The trend of studies on medicaments to prevent and treat dental problems has increased rapidly since 2010, based on data published in PubMed (https://pubmed.ncbi.nlm.nih.gov/). The antibacterial or anti-inflammatory activities of medicament ingredients have been widely examined in previous studies.[1,2] Medicament materials from antibiotics such as ciprofloxacin, metronidazole, and doxycycline,[3] as well as other materials such as calcium hydroxide,[1,3] odontopaste,[3] and quaternary ammonium silane/k21[4] are known to have antibacterial activity.

Wound healing in the oral cavity, including in the tooth sockets, is affected by bacterial and inflammatory activity. Other medicaments that have been studied for wound healing are povidone-iodine (PVP-I) and glycerin (glycerol; GLY). PVP-I has been known to have anti-inflammatory activity, low toxicity, and good tolerability, making it popular in the use of medicaments even though it has been a decade since its first publication.[5] In another study, PVP-I

DOI: 10.20473/j.djmkg.v56.i3.p144–153

and GLY were tested on 347 patients with acute otitis externa (AOE) to analyze their efficacy against the AOE. The clinical trial results showed that AOE treatment with both medicaments has good efficacy and can relieve canal edema and pain in the patient's tragus.[6]

Wound healing is a very complex process involving multiple bioactivities and molecular signaling. Several important bioactivities in wound healing are related to the induction/suppression of inflammation, proliferation, and cell differentiation. The mitogen-activated protein kinase (MAPK) pathway is one of the important signaling pathways associated with these bioactivities.[7] The wound-healing process after a tooth extraction is the same as any other tissue-healing process; that is, it is complex and dynamic. Restoration of damaged tissue integrity involves cellular components and an extracellular matrix (ECM).[8] However, research on medicaments for molecular wound healing is still rare, necessitating the current study. Ovalbumin, the main component in chicken eggs (*Gallus domesticus*), makes up more than 50% of all protein components in eggs. Molecularly, ovalbumin (SERPINB14) is a protein with a molecular weight of 45 kDa with 385 amino acids and is a part of the large Serpin group (the serpin superfamily). Based on the amino acid sequence (aa), there is 1 disulfide bond linking Cys74 and Cys121, with half of the residues being hydrophobic and one-third being acidic.[9,10] Ovalbumin is known to play a role as a carrier protein that can increase the antioxidant effect and solubility of curcumin.[11] However, there is still limited information related to its proliferative activity. Therefore, this study aims to examine the potential of ovalbumin as a wound-healing medicament in tooth extraction sockets by induction of cell proliferation through the ERK/MAPK signaling compared to PVP-I and GLY in silico.

MATERIALS AND METHODS

Protein structures of ovalbumin (UniProt ID: P01012) and extracellular signal-regulated kinase2 (ERK2) (PDB ID: 5V60) were downloaded from the UniProt database (https://www.uniprot.org/) in FASTA format for ovalbumin and from the RCSB PBD (https://www.rcsb.org/) in PDB format for ERK2. The molecules used were PVP-I (CID: 11989721), GLY (CID: 753), and ATP-analogue (adenosine 5'-[β,γ-methylene]triphosphate [AMP-PCP]) (CID: 91532), which were downloaded in .sdf format from PubChem (https://pubchem.ncbi.nlm.nih.gov/). Prediction of ovalbumin peptide bioactivity was carried out via the BIOPEP-UWM web server (http://www.uwm.edu.pl/biochemia/index.php/en/biopep).[12]

Then, ovalbumin was hydrolyzed by the extracellular protease enzymes chymotrypsin (EC 3.4.21.1), trypsin (EC 3.4.21.4), and pepsin, pH 1.3 (EC 3.4.23.1) using the BIOPEP-UWM web server, which resulted in 141 fragments.[8] The fragments were selected based on how many active peptides are in the fragment sequence and the bioactivity of those peptides based on the BIOPEP-UWM database. After that, six fragments were selected that had peptides with anti-inflammatory-related bioactivity, including anti-inflammatory and antioxidant activity.

Six of the selected fragments were converted to Simplified Molecular Input Line Entry System (SMILES) via NovoProlabs (https://www.novoprolabs.com/tools/convert-peptide-to-smiles-string). Next, each SMILES fragment was loaded onto the Similarity Ensemble Approach (SEA) (https://sea.bkslab.org/) and SuperPred (https://prediction.charite.de/subpages/target_prediction.php) webservers to obtain protein prediction targets.[13,14] The cut off chosen from the SEA results was max Tc > 0.5, and SuperPred had a probability > 90%. Then, from the prediction results, ≥ 70 target proteins were obtained. The target protein was inputted into STRING (https://string-db.org/) to see the bioactivity of the target protein.[15] The setting used was a "physical" type network that showed "confidence" through the thickness of the line with high confidence criteria (0.700). The target protein without interaction was eliminated so that 29 target proteins remained.

The selected target proteins (29 proteins) were downloaded from STRING and analyzed using Cytoscape ver. 3.9.1 (Cytoscape Consortium) and the GOlorize plugin.[16,17] First, the protein network was analyzed using the NetworkAnalyzer to obtain data betweenness and closeness centrality and degree.[18] Then, the network was analyzed by gene ontology (GO) using the GOlorize plugin, which generated GO data related to proteins in the tissue and colored protein nodes in the tissue according to their bioactivity. Furthermore, bioactivities related to wound healing including regulation of proliferation, angiogenesis, growth factor production, and anti-inflammatory[19] were selected for further study.

Six fragments (fragment 1 to fragment 6), PVP-I (CID: 11989721), GLY (CID: 753), and AMP-PCP (ATP-analogue) (CID: 91532), were used for molecular docking analysis with the predicted protein. The selected target protein had average value betweenness centrality (BC) and the highest predictive value of all fragments with PVP-I (CID: 11989721) and GLY (CID: 753) as controls. Furthermore, the second docking was carried out to examine the effect of the fragments on the interaction of ATP with MAPK1. The second docking was carried out between AMP-PCP (CID: 91532) and MAPK1 (ERK2) (PDB ID: 5V60) with the previous six ovalbumin fragment ligands. Molecular docking was carried out using Autodock Vina on PyRx 0.9.7 with ligands that were minimized in energy through the Open Babel plugin and proteins that were removed by water molecules and ligands using Biovia Discovery Studio ver 19.1.0.18287.[20] Finally, visualization was carried out with Biovia Discovery Studio ver 19.1.0.18287 to visualize the interaction between fragments and the AMP-PCP (ATP-analogue) to ERK2.

Statistical analysis was conducted to validate the results of the docking analysis, which presented standard

DOI: 10.20473/j.djmkg.v56.i3.p144–153

deviations. The analysis was conducted using GraphPad Prism9 with a one-way ANOVA followed by Tukey's multiple comparisons test.

RESULTS

The ovalbumin peptide fragments obtained were 142 fragments from 141 sites cut by the selected enzymes. This hydrolysis model used independent variables in the form of the number and type of enzymes, where the following fragments were the result of the activity of chymotrypsin (EC 3.4.21.1); trypsin (EC 3.4.21.4); and pepsin, pH 1.3 (EC 3.4.23.1), which acted at the same time. There were 50 fragments with one amino acid (phenylalanine, histidine, lysine, methionine, asparagine, arginine, tryptophan, and tyrosine), 38 and 20 fragments with two and three amino acids, 18 and 3 fragments with four and five amino acids, and 13 fragments with more than 5 amino acids, one of those was composed of 19 amino acids (Table 1).

Furthermore, to analyze the fragment's potential bioactivity related to cell proliferation, we used ovalbumin's active peptide database, which has antioxidant and anti-inflammatory bioactivity. The active peptide was then used to determine which fragments had the same peptide composition. Next, 142 fragments were reduced to six active fragments: AAH (Fragment 1/F1), EL (F2), GSIGAASM (F3), GIIR (F4), TSVL (F5), and VY (F6) (Table 2). The six fragments were predicted to interact with a total of 74 proteins, and five proteins—CAPN1 (calpain-1 catalytic subunit), CFB (complement factor B), FOHL1 (folate hydrolase 1), Human leukocyte antigens class I histocompatibility antigen (HLA-A), and N-acetylated-alpha-linked acidic dipeptidase 2 (NAALAD2)—were predicted to interact with two fragments. Meanwhile, PVP-I and GLY were predicted not to form interactions with any proteins based on the SEA target prediction.

The next protein prediction was conducted using SuperPred to obtain additional prediction results from other

Table 1. Fragment peptide ovalbumin (UniProt ID: P01012) after hydrolysis through BIOPEP-UWM

Sequence	Location	Sequence	Location	Sequence	Location	Sequence	Location
M	[1-1]	SL	[101-102]	VTEQ ESK	[201-207]	EEK	[289-291]
GSIGAASM	[2-9]	ASR	[103-105]	PVQM	[208-211]	Y	[292-292]
EF	[10-11]	L	[106-106]	M	[212-212]	N	[293-293]
CF	[12-13]	Y	[107-107]	Y	[213-213]	L	[294-294]
DVF	[14-16]	AEER	[108-111]	QIGL	[214-217]	TSVL	[295-298]
K	[17-17]	Y	[112-112]	F	[218-218]	M	[299-299]
EL	[18-19]	PIL	[113-115]	R	[219-219]	AM	[300-301]
K	[20-20]	PEY	[116-118]	VASM	[220-223]	GITDVF	[302-307]
VH	[21-22]	L	[119-119]	ASEK	[224-227]	SSSAN	[308-312]
H	[23-23]	QCVK	[120-123]	M	[228-228]	L	[313-313]
AN	[24-25]	EL	[124-125]	K	[229-229]	SGISS AESL	[314-322]
EN	[26-27]	Y	[126-126]	IL	[230-231]	K	[323-323]
IF	[28-29]	R	[127-127]	EL	[232-233]	ISQAVH	[324-329]
Y	[30-30]	GGL	[128-130]	PF	[234-235]	AAH	[330-332]
CPIAIM	[31-36]	EPIN	[131-134]	ASGTM	[236-240]	AEIN	[333-336]
SAL	[37-39]	F	[135-135]	SM	[241-242]	EAGR	[337-340]
AM	[40-41]	QTAAD QAR	[136-143]	L	[243-243]	EVVGSA EAGVDA	[341-359]
VY	[42-43]	EL	[144-145]	VL	[244-245]	ASVSEEF R	[360-360]
L	[44-44]	IN	[146-147]	L	[246-246]	ADH	[361-363]
GAK	[45-47]	SW	[148-149]	PDEV SGL	[247-253]	PF	[364-365]
DSTR	[48-51]	VESQTN	[150-155]	EQL	[254-256]	L	[366-366]
TQIN	[52-55]	GIIR	[156-159]	ESIIN	[257-261]	F	[367-367]
K	[56-56]	N	[160-160]	F	[262-262]	CIK	[368-370]
VVR	[57-59]	VL	[161-162]	EK	[263-264]	H	[371-371]
F	[60-60]	QPSSV DSQTAM	[163-173]	L	[265-265]	IATN	[372-375]
DK	[61-62]	VL	[174-175]	TEW	[266-268]	AVL	[376-378]
L	[63-63]	VN	[176-177]	TSSN	[269-272]	F	[379-379]
PGF	[64-66]	AIVF	[178-181]	VM	[273-274]	F	[380-380]
GDSIEAQ CGTSVN	[67-79]	K	[182-182]	EER	[275-277]	GR	[381-382]
VH	[80-81]	GL	[183-184]	K	[278-278]	CVSP	[383-386]
SSL	[82-84]	W	[185-185]	IK	[279-280]		
R	[85-85]	EK	[186-187]	VY	[281-282]		
DIL	[86-88]	AF	[188-189]	L	[283-283]		
N	[89-89]	K	[190-190]	PR	[284-285]		
QITK	[90-93]	DEDTQAM	[191-197]	M	[286-286]		
PN	[94-95]	PF	[198-199]	K	[287-287]		
DVY	[96-98]	R	[200-200]	M	[288-288]		
SF	[99-100]						

DOI: 10.20473/j.djmkg.v56.i3.p144–153

Table 2. Prediction of active peptide ovalbumin (UniProt ID: P01012) with anti-inflammatory and antioxidant bioactivity

Active Peptides	Sequence Location	Active Peptides	Sequence Location	Active Fragment	Sequence Location
AEERYP	[110-115]	LW	[190-191]	A**AH**	[340-342]
AH	[341-342]	LWE	[190-192]	**EL**	[18-19], [124-125], [144-145]
DEDTQAMP	[197-204]	LY	[108-109], [129-130]	GSI**GAA**SM	[2-9]
EL	[18-19], [128-129], [148-149], [238-239]	MM	[217-218]	GI**IR**	[160-163]
FC	[11-12], [379-380]	MY	[218-219]	T**SVL**	[303-306]
GAA	[5-7]	NEN	[25-27]	**VY**	[42-43], [281-282]
HH	[22-23]	RY	[113-114]		
IR	[162-163]	SALAM	[37-41]		
KD	[47-48], [196-197]	SVL	[304-306]		
KGLWE	[188-192]	VHH	[21-23]		
KP	[95-96], [213-214]	VHHANEN	[21-27]		
LFC[1]	[378-380]	VY	[42-43], [99-100], [289-290]		
LK	[19-20], [332-333]	YLG	[43-45]		
LPF	[239-241]	YNL	[300-302]		

Note: (aa)[1]: amino acid with anti-inflammatory bioactivity. The bold print indicates the amino acids are predicted to be active peptides.

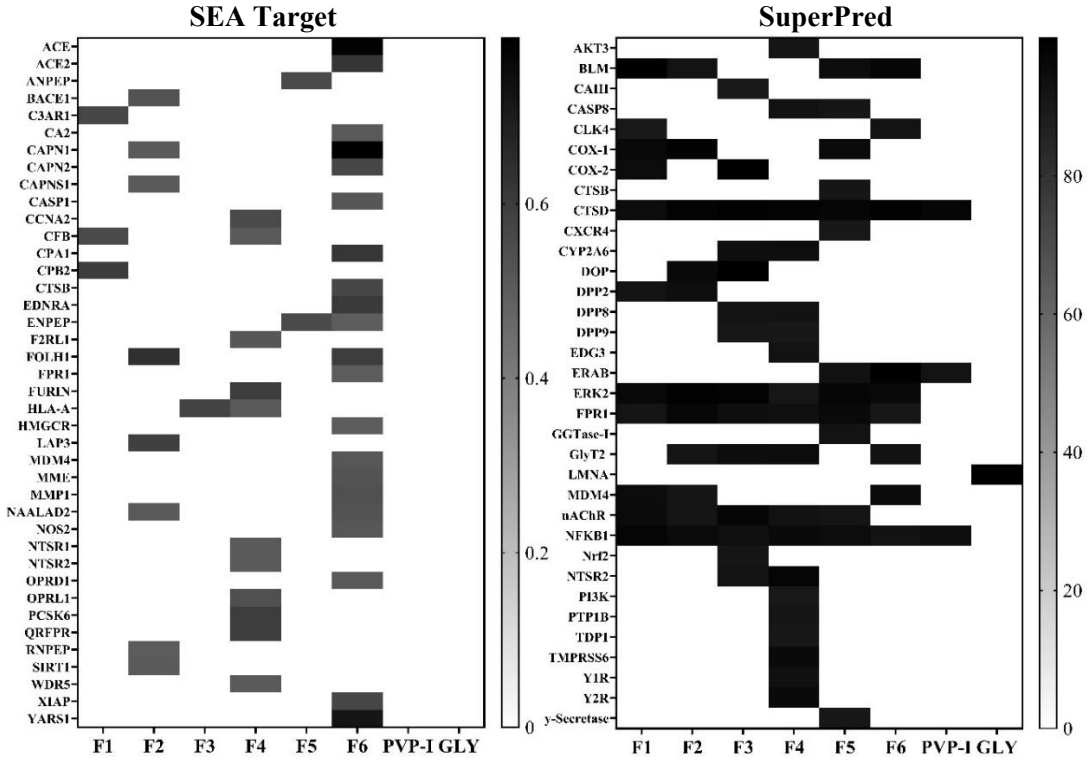

Figure 1. Prediction of target protein for each fragment from SEA target prediction and SuperPred prediction. The target proteins displayed are only those that had a probability value exceeding the specified cutoff (SEA target prediction, cutoff maxTc ≥ 0.5; SuperPred, cutoff probability ≥ 90%). The black color of the squares corresponds to the increase in the probability score.

DOI: 10.20473/j.djmkg.v56.i3.p144–153

databases and increase the probability of approaching the real condition. A total of 34 proteins were predicted to interact with six fragments and control drugs. PVP-I was predicted to interact with CTSD, ERAB, and NFKB1, whereas GLY was predicted to interact with lamin A/C (LMNA; Figure 1). Next, 30 proteins from the enrichment process were obtained and arranged according to the value of BC. BC was obtained from the protein interaction network. The higher the BC score, the more important the role of the protein in the network.[18] The target protein for docking analysis was selected from the previous 29 proteins with the highest BC and MaxTC/probability scores (Figure 2; Table 3). ERK2 was chosen as a protein target for molecular docking analysis because it is known to interact with all fragments based on SuperPred predictions, and it has a BC score of 0.14 with a mean probability of 72.19% to interact with all ligands. Then, based on GO analysis, ERK2 had a role in the processes of proliferation and cell survival. It would be interesting to study further the effect of the ovalbumin fragment in influencing the interaction of ERK2 with its downstream protein.

Hereafter, bioactivity analysis based on the interactions of 59 proteins demonstrates the presence of bioactivity, and Table 4 shows associated proteins. The three biological activities of the selected ontology genes had different confidence and strength scores. The confidence score used was the p-value score and Bonferroni's corrected p-value to increase the credibility of the results. Based on Bonferroni's p-value and corrected p-value scores,[21] the three bioactivities had a score of < 0.05, meaning they had a probability of occurring. Positive regulation of cell proliferation was the most potent bioactivity, followed by

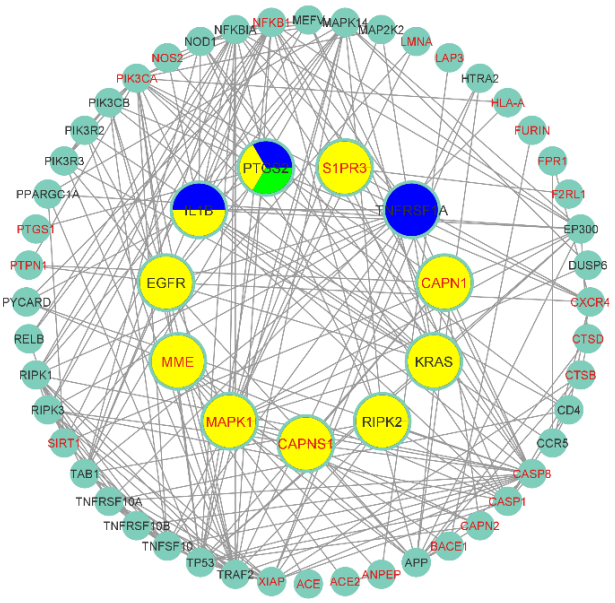

Figure 2. Protein network associated with previously predicted proteins. A total of 59 proteins (29 predicted proteins [red label] and 30 enrichment proteins) were obtained. Yellow-colored proteins indicate positive regulation of cell proliferation (GO-ID: 8284) bioactivity, blue-colored proteins indicate positive regulation of angiogenesis (GO-ID: 45766) bioactivity, and green-colored proteins indicate positive regulation of fibroblast growth factor production (GO-ID: 90271) bioactivity.

Table 3. Betweenness centrality score in the highest PPI and probability

Name	Betweenness Centrality Score	Probability Mean (%)
APP	0.26	0
MAPK1	0.14	72.19
MME	0.13	0
EGFR	0.11	15.16
CASP8	0.10	23.01
PIK3CA	0.08	11.25
TP53	0.08	0
IL1B	0.08	0
NFKB1	0.07	82.91
NFKBIA	0.06	0
MAPK14	0.05	0
CXCR4	0.04	11.31
EP300	0.04	41.34
PTGS2	0.04	0
TRAF2	0.04	0

Note: The proteins in bold are among the 29 proteins selected from the previous analysis (Figure 1). Some proteins have an average probability of 0% because they are not predicted to interact with any fragments during target prediction analysis.

Table 4. Prediction of bioactivity of 59 proteins based on functional annotation gene ontology analysis

GO-ID	Description	P-Value	Corrected P-Value	Gene
8284	Positive regulation of cell proliferation	1.6103E-5	1.6163E-4	CAPNS1 MME RIPK2 IL1B MAPK1 S1PR3 KRAS CAPN1 PTGS2 EGFR
45766	Positive regulation of angiogenesis	7.3175E-4	3.7681E-3	IL1B PTGS2 TNFRSF1A
90271	Positive regulation of fibroblast growth factor production	4.1250E-3	1.4003E-2	PTGS2

DOI: 10.20473/j.djmkg.v56.i3.p144–153

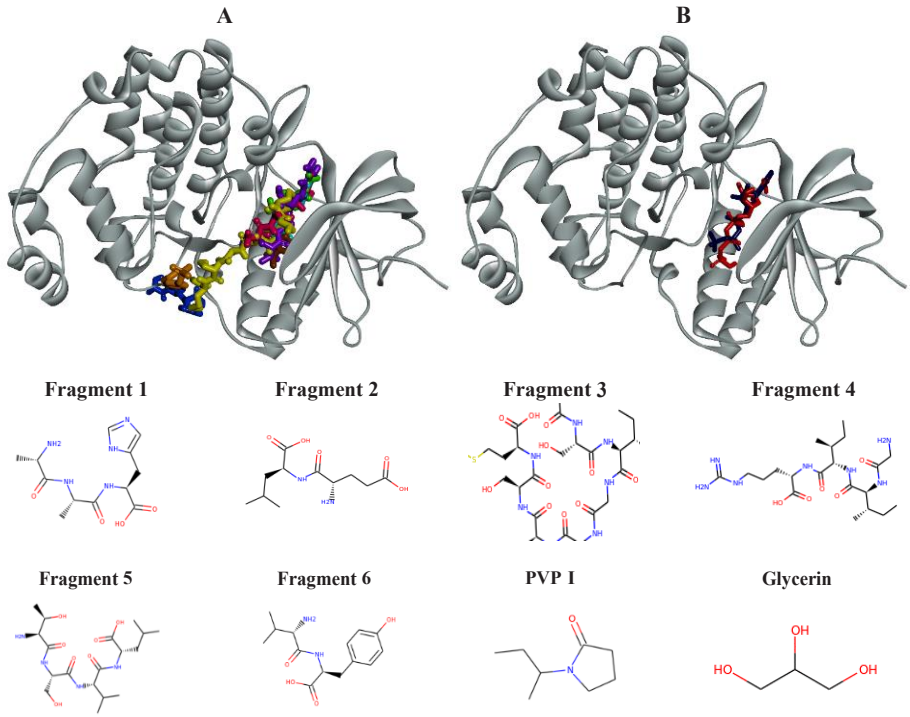

Figure 3. The location of the six fragments interacting with ERK2 at the ATP phosphorylation site. (A) The location of the six fragments, F1 = blue, F2 = green, F3 = yellow, F4 = purple, F5 = pink, F6 = turquoise, GLY = orange, and PVP-I = brown. (B) Location of ATP phosphorylation at the ERK2 phosphorylation site. Comparison of AMP-PCP (CID: 91532) against original (native) AMP-PCP. The two ligands were juxtaposed to justify the similarity of the positions and interactions formed. (Blue) AMP-PCP (ATP-analogue) interacts at the phosphorylation site of ERK2 according to the study of Lechtenberg et al.[22] (GDP ID: 5V60). (Red) AMP-PCP control (CID: 91532).

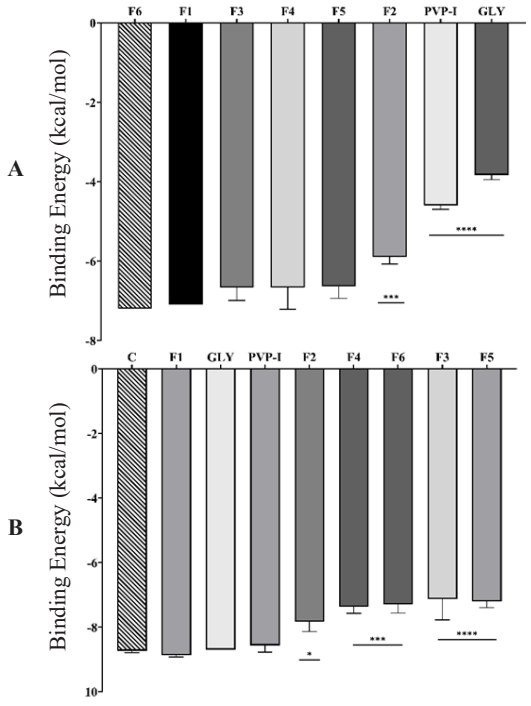

Ligand	Binding Energy (kcal/mol)
F1	-7.10 ± 0.00
F2	-5.90 ± 0.17
F3	-6.67 ± 0.32
F4	-6.67 ± 0.55
F5	-6.63 ± 0.30
F6	-7.20 ± 0.00
GLY	-3.83 ± 0.11
PVP-I	-4.60 ± 0.10

ERK2 + Ligand	Binding Energy (kcal/mol)
C	-8.73 ± 0.06
F1	-8.87 ± 0.06
F2	-7.83 ± 0.31
F3	-7.13 ± 0.64
F4	-7.37 ± 0.21
F5	-7.20 ± 0.20
F6	-7.30 ± 0.26
GLY	-8.70 ± 0.00
PVP-I	-8.57 ± 0.21

Figure 4. Comparison of the binding energy scores of fragments and compounds. (A) Comparison of binding energy scores of all ligands against F6, which had the lowest binding energy score. One-way ANOVA ($p < .05$); ***p =.0004, ****p < .0001. (B) The AMP-PCP binding energy score against ERK2, which interacted with all ligands, was compared with the AMP-PCP binding energy score against the control ERK2 (C). One-way ANOVA ($P < .05$); *p = .0216, ***p < .001, ****p < .0001.

DOI: 10.20473/j.djmkg.v56.i3.p144–153

positive regulation of angiogenesis and fibroblast growth factor (FGF) production.

Next are the results related to molecular docking analysis. The ATP-binding site or phosphorylation site of ERK2 (PDB ID: 5V60) was found in amino acids 31-39 and 54, including ILE31, GLY32, GLU33, GLY34, ALA35, TYR36, GLY37, MET38, VAL39, and LYS54.[22] The six fragments were docked blindly to find out where the optimal location of interaction would occur in each ligand. Docking was carried out in three replications with different coordinates. Replication coordinates 1, center: X: -4.591, Y: 8,733, Z: 47,759; dimension (angstrom): X: 79,999, Y: 49,579, Z: 63,872. Replication 2, center: X: -2.857, Y: 6.812, Z: 46.304; dimension (angstrom): X: 64,739, Y: 48,945, Z: 70,444. Replication 3, center: X: -3,270, Y: 6,527, Z: 46,102; dimension (angstrom): X: 66,329, Y: 50,285, Z: 70,678. F6 required the least amount of binding energy (interaction energy), followed by F1. From these results, it can be concluded that the interaction between F1 and GLY, which is outside the ATP phosphorylation site, may affect the molecular bioactivity of ERK2 without having to compete with ATP. At the same time, the interaction between F2, F3, F4, F5, F6 and PVP-I may act as an inhibitor of ATP phosphorylation on ERK2 (Figure 3).

The second docking was carried out by interacting AMP-PCP (ATP analogue) as a native experimental ligand with ERK2 to evaluate the interaction docked with the previous ligand. The docking procedure was the same as in the previous step in triplicate, with the original AMP-PCP ligand anchored to ERK2 (AMP-PCP original) (PDB ID: 5V60) substituted with AMP-PCP (CID: 91532) anchored to ERK2 (PDB ID: 5V60), which was prepared as a control. Replication coordinates 1, center: X: 14,533, Y: 13,085, Z: 15,442; dimension (angstrom): X: 25,607, Y: 29.3, Z: 36,223. Replication 2, center: X: 13,998, Y: 10,744, Z: 15,947; dimension (angstrom): X: 30,065, Y: 25,309, Z: 28,456. Replication 3, center: X: 13,658, Y: 11,993, Z: 15,166; dimension (angstrom): X: 27,266, Y: 25,481, Z: 25,573. According to the second docking result, F1 interaction can reduce AMP-PCP binding energy to ERK2 by 0.01% compared to the control (Figure 4). A visualization was carried out to understand in detail the interactions that occurred between the ligand and ERK2. The visualization of AMP-PCP control and original AMP-PCP in the ERK2 ligand (PDB ID: 5V60) aims to validate the AMP-PCP pose after re-docking (Figure 5). Table 5 is the list of all residues that interacted with the ligand.

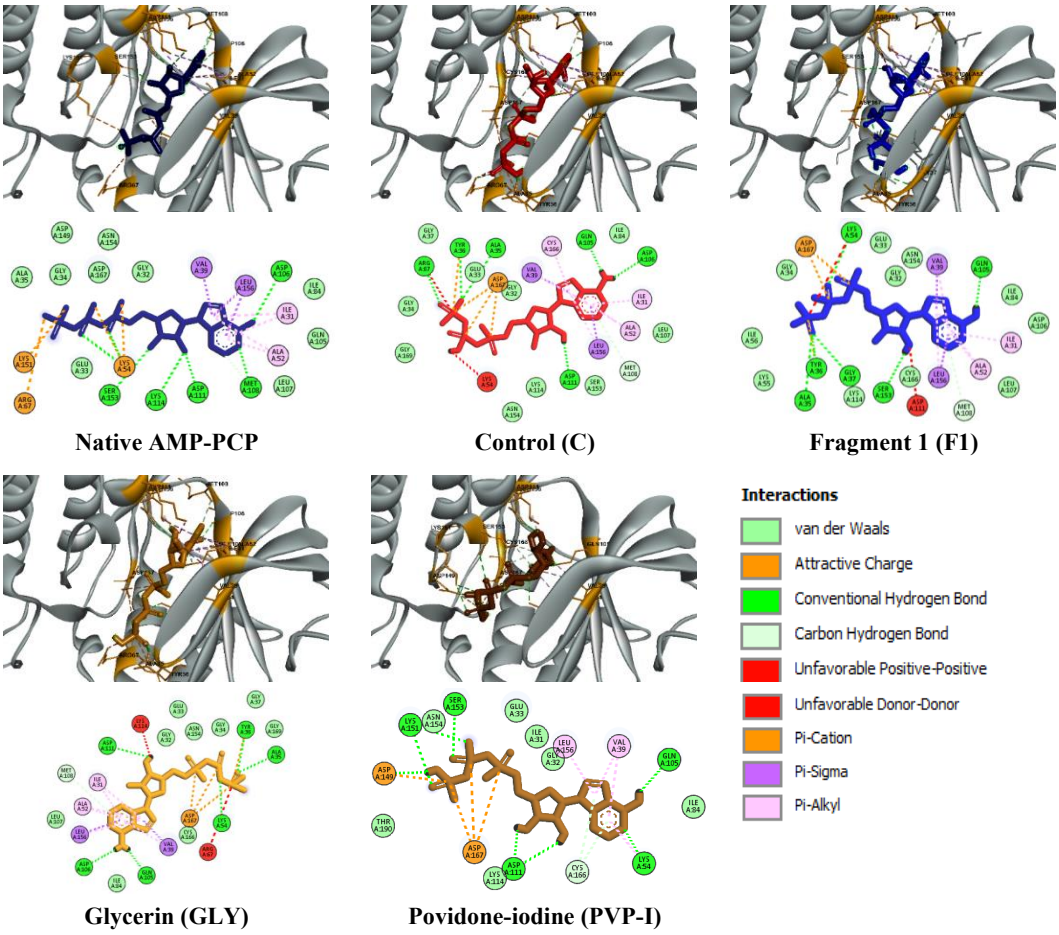

Figure 5. The interaction between AMP-PCP and ERK2 with F1, GLN, and PVP-I.

DOI: 10.20473/j.djmkg.v56.i3.p144–153

Table 5. Residues that form interactions with AMP-PCP

	Native ERK2/AMP-PCP	ERK2 Control	ERK2/F1 – AMP-PCP	ERK2/GLY – AMP-PCP	ERK2/PVP-I – AMP-PCP
Hydrogen bond	LYS54 LYS54 ASP106 MET108 MET108 ASP111 LYS114 SER153 SER153	ALA35 TYR36 ARG67 GLN105 ASP106 MET108 ASP111	ALA35 TYR36 GLY37 LYS54 GLN105 MET108 SER153	ALA35 TYR36 LYS54 GLN105 ASP106 MET108 ASP111	LYS54 GLN105 ASP111 ASP111 ASP149 LYS151 LYS151 SER153 CYS166 CYS166
Electrostatic bond	LYS54 LYS54 ARG67 LYS151	TYR36 ASP167 ASP167 ASP167	TYR36 ASP167 ASP167	TYR36 ASP167 ASP167 ASP167	ASP149 ASP167 ASP167 ASP167
Hydrophobic bond	ILE31 VAL39 ALA52 LEU156 LEU156	ILE31 VAL39 VAL39 ALA52 ALA52 LYS54 ARG67 LEU156 LEU156	ILE31 VAL39 VAL39 VAL39 ALA52 ALA52 ALA52 LEU156 LEU156 LEU156	ILE31 ILE31 VAL39 VAL39 VAL39 ALA52 ALA52 ALA52 LEU156 LEU156	VAL39 VAL39 ALA52 LYS54 LEU156
Van der Waals bond	GLY32 GLU33 GLY34 ALA35 ILE84 GLN105 LEU107 ASP149 ASN154 ASP167	GLY32 GLU33 GLY34 GLY37 ILE84 LEU107 LYS114 SER153 ASN154 GLY169	GLY32 GLU33 GLY34 LYS55 ILE56 ILE84 ASP106 LEU107 LYS114 ASN154 CYS166	GLY32 GLU33 GLY34 GLY37 ILE84 LEU107 ASN154 CYS166 GLY169	ILE31 GLY32 GLU33 ILE84 LYS114 ASN154 THR190
Unfavorable bond			LYS54 LYS54 ARG67 ASP111	LYS54 LYS54 ARG67 ARG67 ASP111 LYS114	LYS54 LYS54 ARG67 ASP111

DISCUSSION

Tooth extraction is an activity that causes injury to the tooth socket because of the presence of parts of the gums and nerves that interact directly with the environment (the oral cavity). Pathogenic microorganisms can enter the wound, causing the body to automatically respond with inflammation and the wound-healing process.[23] Wound healing is a very complex process in the human body. It involves various types of cells and ranges from repair and arrangement of specialized structures, such as collagen, migration, proliferation, and differentiation of cells.[19,24]

In this study, we report potential bioactivity that positively regulates cell proliferation (GO-ID: 8284), angiogenesis (GO-ID: 45766), and FGF production (GO-ID: 90271) by proteins targeted by an ovalbumin fragment. These three bioactivities are known to play a crucial role in the proliferative phase compared to the inflammatory phase or the maturation (remodeling) phase in the wound-healing process. In the inflammatory phase, the process of vascular vessel contraction and blood clotting is followed by an increase in the number of leukocytes in the wound tissue, including an increase in the number of neutrophils due to an increase in pro-inflammatory cytokines such as interleukin-1, tumor necrosis factor-alpha (TNF-α), and interferon-gamma and chemotactic agents such as pathogen-specific associated molecular pattern, damage-associated molecular pattern, complement, histamine, prostaglandins, and leukotrienes. In addition to neutrophils, there is also an increase in the macrophage population due

DOI: 10.20473/j.djmkg.v56.i3.p144–153

to the chemotactic compounds tumor growth factor-beta (TGF-β) and monocyte chemoattractant protein-1.[19,24]

Furthermore, in the proliferative phase, there are re-epithelialization, neovascularization (angiogenesis), and immunomodulators aimed at repairing and restructuring damaged tissue. In this phase, tissue granulation occurs by fibroblasts, which play an important role in inducing the formation of a new ECM and blood vessels. Another process that is no less important is angiogenesis and vasculogenesis (neovascularization), which aims to form new blood vessels that will supply nutrients and maintain oxygen homeostasis in the healing process in injured tissues. This process is inseparable from the presence of pro-angiogenic signals such as vascular endothelial growth factor (VEGF), FGF, platelet-derived growth factor beta, TGF-β, and angiopoietins. The last involves the formation of pericytes, which play a role in microvascular stability, regulation of blood flow, and the formation of vascular protection from bacteria.[25] The last phase is maturation (remodeling), which causes contraction of the wound and replacement of type-III collagen with type-I collagen.[24]

The three bioactivities are obtained from a network of 59 proteins where amyloid-β precursor protein (APP), MAPK1 (ERK2), MME, epithelial growth factor receptor (EGFR), and caspase-8 (CASP8) are important links in the network. In wound healing, APP plays an important role in the proliferation, migration, and adhesion of endothelial cells. Endothelial cells require APP as a mediator of the Scr/FAK pathway in VEGF signaling.[26] Furthermore, in regard to ERK2, upregulation, and phosphorylation of ERK1/2 and AKT are known to be consistent with increased proliferation and migration of human skin fibroblasts and human umbilical vein endothelial cells in vitro due to sea cucumber peptide treatment.[27] Other studies have also shown that the activation of the EGFR/MEK/ERK signaling pathway by the SOX2 gene is known to accelerate wound healing through the induction of keratinocyte cell migration and proliferation.[28] Meanwhile, the inhibition of corneal MME is known to improve corneal epithelial wound healing in mice.[29] Eliminating CASP8 is known to increase the proliferation and migration of human epidermal keratinocytes, which can promote wound healing in mice.[30]

Molecular docking analysis results show that peptide fragments VY (F6), AAH (F1), GSIGAASM (F3) and require the lowest binding energy. Interestingly, the molecular docking results blindly show two interaction sites outside and inside the ATP phosphorylation site. Then, according to the molecular docking results of the AMP-PCP interaction with ERK2, F1 has the potential to reduce the binding energy of the AMP-PCP interaction with ERK2 in the phosphorylation domain, although the difference is not significant. The interaction of F1 outside the phosphorylation site minimizes the probability that F1 will compete with ATP. Additionally, the interaction of GLY and PVP-I on ERK2 increases the binding energy of AMP-PCP when it interacts with ERK2, although the difference is again not significant. What is interesting about the interaction between the two is the different interaction sites, where GLY interacts outside the ATP phosphorylation site and PVP-I acts inside the phosphorylation site. Based on its location and required binding energy, PVP-I has the potential to be an inhibitor of ATP phosphorylation on ERK2 when it has interacted with ERK2 first. However, the binding energy required for GLY and PVP-I to interact with ERK2 is high, so further research is needed to obtain more comprehensive conclusions.

Furthermore, PVP-I is known to have anti-inflammatory activity through suppression of TNF- expression in human neutrophil cells in vitro[31] and decreased galactosidase activity in E. coli cultures[32] so that it can reduce the level of interleukin-6, TNF-α, and rheumatoid factor in the serum of rheumatoid arthritis patients.[33] GLY is more often used as a viscous mixing agent with a heavy molecular weight, such as a Ca^{2+} and OH^- mixer for intracanal $Ca(OH)_2$ medicaments.[34] Furthermore, the sodium alginate (NaAlg)-PVP-I complex is known to have a wound-healing effect by accelerating the closure process.[35] Structurally, PVP-I is composed of a polyvinyl pyrrolidone (povidone) polymer complex with elemental iodine, which is intended for health practitioners. Various studies on PVP-I have shown anti-inflammatory, anti-bacterial, anti-biofilm, anti-edema, and hemostatic activity; low toxicity; and good tolerability. Thus, it is still used as a medicament even though it has been more than a decade since its development.[5,31] Ovalbumin was found to affect the interaction of ERK2 and AMP-PCP in this study. Ovalbumin is also predicted to have the potential to be an additional medicament/component complex for better wound healing than PVP-I and GLY.

In conclusion, ovalbumin has the potential to induce cell proliferation by decreasing the binding energy required for AMP-PCP to interact with ERK2 compared to GLY and PVP-I, which slightly increase the binding energy required for AMP-PCP to interact with ERK2. Further in vitro/in vivo development and testing are needed to validate and develop ovalbumin as a pro-proliferative medicament.

REFERENCES

1. Athanassiadis B, Walsh LJ. Aspects of solvent chemistry for calcium hydroxide medicaments. Materials (Basel). 2017; 10(10): 1219.
2. Manohar M, Sharma S. A survey of the knowledge, attitude, and awareness about the principal choice of intracanal medicaments among the general dental practitioners and nonendodontic specialists. Indian J Dent Res. 2018; 29(6): 716–20.
3. Govindaraju L, Jenarthanan S, Subramanyam D, Ajitha P. Antibacterial activity of various intracanal medicament against Enterococcus faecalis, Streptococcus mutans and Staphylococcus aureus: An In vitro study. J Pharm Bioallied Sci. 2021; 13(5): 157–61.
4. Kok ESK, Lim XJ, Chew SX, Ong SF, See LY, Lim SH, Wong LA, Davamani F, Nagendrababu V, Fawzy A, Daood U. Quaternary ammonium silane (k21) based intracanal medicament triggers biofilm destruction. BMC Oral Health. 2021; 21(1): 116.
5. Bigliardi PL, Alsagoff SAL, El-Kafrawi HY, Pyon J-K, Wa CTC, Villa MA. Povidone iodine in wound healing: A review of current concepts and practices. Int J Surg. 2017; 44: 260–8.

DOI: 10.20473/j.djmkg.v56.i3.p144–153

6. Patel M, Dehadaray A. Povidone-iodine and glycerine for treatment of acute otitis externa. Saudi J Heal Sci. 2018; 7(3): 178–82.
7. Sun Y, Liu W-Z, Liu T, Feng X, Yang N, Zhou H-F. Signaling pathway of MAPK/ERK in cell proliferation, differentiation, migration, senescence and apoptosis. J Recept Signal Transduct. 2015; 35(6): 600–4.
8. Velnar T, Bailey T, Smrkolj V. The wound healing process: An overview of the cellular and molecular mechanisms. J Int Med Res. 2009; 37(5): 1528–42.
9. Fatoki TH, Aluko RE, Udenigwe CC. In silico investigation of molecular targets, pharmacokinetics, and biological activities of chicken egg ovalbumin protein hydrolysates. J Food Bioact. 2022; 17: 34–48.
10. Chay Pak Ting BP, Pouliot Y, Gauthier SF, Mine Y. Fractionation of egg proteins and peptides for nutraceutical applications. In: Separation, Extraction and Concentration Processes in the Food, Beverage and Nutraceutical Industries. Elsevier; 2013. p. 595–618.
11. Liu Y, Ying D, Cai Y, Le X. Improved antioxidant activity and physicochemical properties of curcumin by adding ovalbumin and its structural characterization. Food Hydrocoll. 2017; 72: 304–11.
12. Minkiewicz, Iwaniak, Darewicz. BIOPEP-UWM database of bioactive peptides: Current opportunities. Int J Mol Sci. 2019; 20(23): 5978.
13. Keiser MJ, Roth BL, Armbruster BN, Ernsberger P, Irwin JJ, Shoichet BK. Relating protein pharmacology by ligand chemistry. Nat Biotechnol. 2007; 25(2): 197–206.
14. Nickel J, Gohlke B-O, Erehman J, Banerjee P, Rong WW, Goede A, Dunkel M, Preissner R. SuperPred: update on drug classification and target prediction. Nucleic Acids Res. 2014; 42(W1): W26–31.
15. Szklarczyk D, Gable AL, Lyon D, Junge A, Wyder S, Huerta-Cepas J, Simonovic M, Doncheva NT, Morris JH, Bork P, Jensen LJ, Mering C von. STRING v11: protein–protein association networks with increased coverage, supporting functional discovery in genome-wide experimental datasets. Nucleic Acids Res. 2019; 47(D1): D607–13.
16. Garcia O, Saveanu C, Cline M, Fromont-Racine M, Jacquier A, Schwikowski B, Aittokallio T. GOlorize: a Cytoscape plug-in for network visualization with Gene Ontology-based layout and coloring. Bioinformatics. 2007; 23(3): 394–6.
17. Shannon P, Markiel A, Ozier O, Baliga NS, Wang JT, Ramage D, Amin N, Schwikowski B, Ideker T. Cytoscape: A software environment for integrated models of biomolecular interaction networks. Genome Res. 2003; 13(11): 2498–504.
18. Xia J, Benner MJ, Hancock REW. NetworkAnalyst - integrative approaches for protein–protein interaction network analysis and visual exploration. Nucleic Acids Res. 2014; 42(W1): W167–74.
19. Gonzalez AC de O, Costa TF, Andrade Z de A, Medrado ARAP. Wound healing - A literature review. An Bras Dermatol. 2016; 91(5): 614–20.
20. Dallakyan S, Olson AJ. Small-molecule library screening by docking with PyRx. In: Hempe JE, Williams CH, Hong CC, editors. Chemical Biology Methods and Protocols. New York: Humana Press; 2015. p. 243–50.
21. Jafari M, Ansari-Pour N. Why, When and How to adjust your P values? Cell J. 2019; 20(4): 604–7.
22. Lechtenberg BC, Mace PD, Sessions EH, Williamson R, Stalder R, Wallez Y, Roth GP, Riedl SJ, Pasquale EB. Structure-guided strategy for the development of potent bivalent ERK inhibitors. ACS Med Chem Lett. 2017; 8(7): 726–31.
23. Ningsih JR, Haniastuti T, Handajani J. Re-epitelisasi luka soket pasca pencabutan gigi setelah pemberian gel getah pisang raja (Musa sapientum L) kajian histologis pada marmut (Cavia cobaya). JIKG (Jurnal Ilmu Kedokt Gigi). 2019; 2(1): 1–6.
24. Primadina N, Basori A, Perdanakusuma DS. Proses penyembuhan luka ditinjau dari aspek mekanisme seluler dan molekuler. Qanun Med - Med J Fac Med Muhammadiyah Surabaya. 2019; 3(1): 31–43.
25. Rodrigues M, Kosaric N, Bonham CA, Gurtner GC. Wound healing: A cellular perspective. Physiol Rev. 2019; 99(1): 665–706.
26. Ristori E, Cicaloni V, Salvini L, Tinti L, Tinti C, Simons M, Corti F, Donnini S, Ziche M. Amyloid-β precursor protein APP down-regulation alters actin cytoskeleton-interacting proteins in endothelial cells. Cells. 2020; 9(11): 2506.
27. Zheng Z, Li M, Jiang P, Sun N, Lin S. Peptides derived from sea cucumber accelerate cells proliferation and migration for wound healing by promoting energy metabolism and upregulating the ERK/AKT pathway. Eur J Pharmacol. 2022; 921: 174885.
28. Uchiyama A, Nayak S, Graf R, Cross M, Hasneen K, Gutkind JS, Brooks SR, Morasso MI. SOX2 epidermal overexpression promotes cutaneous wound healing via activation of EGFR/MEK/ERK signaling mediated by EGFR ligands. J Invest Dermatol. 2019; 139(8): 1809-1820.e8.
29. Genova RM, Meyer KJ, Anderson MG, Harper MM, Pieper AA. Neprilysin inhibition promotes corneal wound healing. Sci Rep. 2018; 8(1): 14385.
30. Liu Y, Xiong W, Wang C-W, Shi J-P, Shi Z-Q, Zhou J-D. Resveratrol promotes skin wound healing by regulating the miR-212/CASP8 axis. Lab Investig. 2021; 101(10): 1363–70.
31. Amtha R, Kanagalingam J. Povidone-iodine in dental and oral health: a narrative review. J Int Oral Heal. 2020; 12(5): 407.
32. Lachapelle J-M, Castel O, Casado AF, Leroy B, Micali G, Tennstedt D, Lambert J. Antiseptics in the era of bacterial resistance: a focus on povidone iodine. Clin Pract. 2013; 10(5): 579–92.
33. Su Z, Gao J, Xie Q, Wang Y, Li Y. Possible role of β-galactosidase in rheumatoid arthritis. Mod Rheumatol. 2020; 30(4): 671–80.
34. Putri Kusuma AR. Pengaruh lama aplikasi dan jenis bahan pencampur serbuk kalsium hidroksida terhadap kekerasan mikro dentin saluran akar. ODONTO Dent J. 2016; 3(1): 48–54.
35. Summa M, Russo D, Penna I, Margaroli N, Bayer IS, Bandiera T, Athanassiou A, Bertorelli R. A biocompatible sodium alginate/povidone iodine film enhances wound healing. Eur J Pharm Biopharm. 2018; 122: 17–24.

DOI: 10.20473/j.djmkg.v56.i3.p144–153